RESEARCH ARTICLE | NOVEMBER 01 1992

Three-dimensional instability of strained vortices in a stably stratified fluid

Takeshi Miyazaki; Yasuhide Fukumoto

Phys. Fluids 4, 2515–2522 (1992)
https://doi.org/10.1063/1.858438

Three-dimensional instability of strained vortices in a stably stratified fluid

Takeshi Miyazaki[a)]
National Institute for Environmental Studies, Tsukuba, Ibaraki 305, Japan

Yasuhide Fukumoto
Department of Applied Physics, Nagoya University, Chikusa-ku, Nagoya 464-01, Japan

(Received 2 April 1991; accepted 26 June 1992)

The linear stability of unbounded strained vortices in a stably stratified fluid is investigated theoretically. The problem is reduced to a Floquet problem which is solved numerically. The three-dimensional elliptical instability of Pierrehumbert type [Phys. Rev. Lett. **57**, 2157 (1986)] is shown to be suppressed by the stable stratification and it disappears when the Brunt–Väisälä frequency exceeds unity. On the other hand, two classes of new instability mode are found to occur. One appears only when the Brunt–Väisälä frequency is less than 2, whereas the other persists for all values of the Brunt–Väisälä frequency. The former mode is related to a parametric resonance of internal gravity waves, and the latter modes are related to superharmonic parametric instability.

I. INTRODUCTION

A concentrated vorticity region often appears as a coherent structure in high Reynolds number flows and extensive investigations on its motion and stability have been performed. Three-dimensional (3-D) instability modes are classified into two categories according to their axial wavelengths. One with the longer axial wavelength (much larger than the vortex core radius) is called, after Crow,[1] the Crow instability, who evaluated the Biot–Savart induction velocity to demonstrate that some long wave disturbances on trailing vortices from an aircraft grow exponentially. Widnall, Bliss, and Tsai[2] (WBT) found the instability mode whose axial wavelength is of the order of the core radius and they succeeded in explaining the destabilization of a vortex ring. Recently, Pierrehumbert[3] showed numerically that an unbounded inviscid strained vortex undergoes an instability whose growth rate is independent of wavelength. If the narrow region near the vortex center is considered, the existence of this similar mode implies very short instability. Although the WBT instability and the Pierrehumbert instability seem to be distinguished from each other by their wavelength, they share a common physical mechanism, i.e., resonance between the inertial vortex waves and the locally imposed strain field.[4–8] In fact, the similar continuous instability mode is discretized to be reducible to the WBT instability modes, if an appropriate outer boundary condition is taken into account. It is thus understood that they form the second category which we call the elliptical instability.[7,8]

As for the elliptical instability (our concern focuses on the continuous instability mode of unbounded strained vortices), Bayly[9] formulated the problem as a matrix Floquet problem, which indicated that the instability mode is parametrically excited. Waleffe[7] reduced the problem to an Ince equation and explored its analytical structure thoroughly. He gave, in the limiting case of weak strain, a lucid physical explanation of the instability as a resonant interaction between the inertial wave and the imposed strain field. It is not difficult to incorporate the viscous effect, which was undertaken by Landman and Saffman.[10] They showed that this intrinsically inviscid instability mechanism persists even in the presence of the viscous dissipation.[8,11] Craik[12] proposed to incorporate the contribution of various types of body force and described the influence of a Coriolis force in detail.

Atmospheric and oceanographic fluid motions are subjected to the strong influence of density inhomogeneity associated with temperature and/or salinity variations. Miyazaki and Fukumoto[13] studied the axisymmetric wave propagation along a vertical vortex core in a stably stratified fluid. They showed that a stable stratification has a profound effect on the dispersion relation of inertial vortex waves. This fact strongly suggests that the parametric excitation of instability modes suffers substantial influence, too. Our objective in this paper is to explore the effect of stable stratification on the elliptical instability of Pierrehumbert type.

We formulate the problem in Sec. II, where it is reduced to a Floquet problem following Waleffe.[7] The fluid is assumed to be inviscid, incompressible, nondiffusive, and exponentially stratified. In addition, a somewhat delicate assumption of weak centrifugal force is introduced. The resulting equation for the density variation is a cubic-order Ince equation. The Floquet problem is solved numerically and the stability characteristics are described in Sec. III. Intuitively thinking, the stable stratification acts in the direction to suppress the vertical motion and the three-dimensional instability. This intuition is partly right. The growth rate of the elliptical instability decreases as the stratification becomes more stable and it disappears when the Brunt–Väisälä frequency exceeds unity. More interesting is the appearance of new instability modes. They are classified into two types according to the parameter region where they are observed. The first (we call it the fundamental instability, later), is presented when the Brunt–Väisälä frequency is less than 2 and the other (the super-

[a)]Present address: Department of Mechanical and Control Engineering, University of Electro-Communications, Chofu, Tokyo 182, Japan.

 0899-8213/92/112515-08$04.00

harmonic instability) is found for any positive (nonzero) Brunt–Väisälä frequency. We make, in Sec. IV, an attempt at physical interpretations of the excitation of new instability modes as well as the suppression of the elliptical instability of Pierrehumbert type. It is shown that the new modes are attributed to certain new resonance phenomena. Section V is devoted to summary and discussions.

II. FORMULATION

The fluid is assumed to be inviscid, incompressible, and nondiffusive. The equations of motion are then written in vector form as

$$\rho\left(\frac{\partial \mathbf{u}}{\partial t}+\mathbf{u}\cdot\text{grad}\,\mathbf{u}\right)=-\text{grad}\,p-\rho g\mathbf{e}_z, \tag{1}$$

where $\mathbf{u}=u\mathbf{e}_x+v\mathbf{e}_y+w\mathbf{e}_z$ is the velocity field and ρ and p denote the density and pressure, respectively. The Cartesian coordinates (x, y, z) are used throughout this paper with the corresponding unit vectors $\mathbf{e}_x$, $\mathbf{e}_y$, and $\mathbf{e}_z$. The gravity g acts in the negative z direction. The conditions of incompressibility and nondiffusivity impose

$$\frac{\partial \rho}{\partial t}+\mathbf{u}\cdot\text{grad}\,\rho=0. \tag{2}$$

In consequence, the velocity becomes solenoidal:

$$\text{div}\ \mathbf{u}=0. \tag{3}$$

A. Basic state

We choose, among other general situations, one of the simplest stratification profiles, i.e., the density is exponentially stratified in the z direction. This simplification admits a constant Brunt–Väisälä frequency $N^2=\alpha g/\gamma^2$ throughout the entire fluid, where α is the strength of stable stratification and 2γ denotes the uniform vertical vorticity. The task of constructing the basic steady flow is not so easy, because the centrifugal force produces the pressure and density variations in the horizontal plane and, accordingly, the velocity component in the z direction. In this paper, however, since we confine our attention to the shortest instability mode excited in the neighborhood of the center of an elongated vorticity region, it is reasonable to assume that the centrifugal force is weak compared with the gravity. This ratio is characterized by the Froude number $\text{Fr}=\gamma^2 L/g$, with L being the length scale of interest i.e., the following linear velocity profiles are thought of as a good approximation within the lateral extent L. For typical oceanographic middle-scale vortices, N is order of 10^2 and Fr is order of 10^{-8}. It will not be difficult to conduct a laboratory experiment on vortex motions in a stably stratified fluid, where N is order of unity and Fr is much less than unity (see, for example, Griffiths and Linden[14]). We seek for the steady basic state in the following form of expansions in powers of the small parameter $N^2\,\text{Fr}^2$:

$$U=-\gamma L[(1+\varepsilon)y+O(N^2\,\text{Fr}^2)], \tag{4}$$

$$V=\gamma L[(1-\varepsilon)x+O(N^2\,\text{Fr}^2)], \tag{5}$$

$$W=\gamma L N^2\,\text{Fr}[W_1(x,y)+O(N^2\,\text{Fr}^2)], \tag{6}$$

$$\rho_0=\rho^* e^{-\alpha Lz}[1+N^2\,\text{Fr}^2\rho_1(x,y)+O(N^4\,\text{Fr}^4)], \tag{7}$$

$$P=\frac{\rho^*}{\alpha}ge^{-\alpha Lz}[1+N^2\,\text{Fr}^2 p_1(x,y)+O(N^4\,\text{Fr}^4)], \tag{8}$$

where the space coordinates (x, y, z) are normalized by L and the time by $1/\gamma$. The strength of the rate of strain is represented by ε (<1). The quantities with the subscript 1 are determined, after substituting (4)–(8) into (1) and (2), as

$$p_1=\left(\frac{1-\varepsilon^2}{2}\right)(x^2+y^2), \tag{9}$$

$$\rho_1=\frac{1-\varepsilon^2}{2[N^2-4(1-\varepsilon^2)]}[(N^2-4+4\varepsilon)x^2 + (N^2-4-4\varepsilon)y^2], \tag{10}$$

$$W_1=-\frac{2\varepsilon(1-\varepsilon)(1+\varepsilon)}{N^2-4(1-\varepsilon^2)}xy. \tag{11}$$

It is remarkable that the above expressions (10) and (11) exhibit divergence if the denominator vanishes. (No divergence is presented for $\varepsilon=0$ (axisymmetric) and 1 (simple shear). In the former case, (9) and (10) are the first-order expansion terms of the exact steady state $\rho_0/\rho^*=P\alpha/g\rho^*=\exp[-\alpha Lz+N^2\,\text{Fr}^2(x^2+y^2)/2]$ with no vertical velocity.) The term $2\pi(1-\varepsilon^2)^{-1/2}$ represents the time period in which a fluid particle travels once around the vortex center, whereas $2\pi/N$ is the period of vertical oscillation due to buoyancy. It follows that the divergence takes place when a fluid particle oscillates (with the Brunt–Väisälä frequency) vertically, just twice during one turn around the vortex center. It will be seen below that the same resonance plays an important role in the stability analysis, but we must keep in mind that our approximation deteriorates in the vicinity of this special parameter region $N^2=4(1-\varepsilon^2)$, because we fail to construct the basic state in our framework.

B. Linear disturbances

We consider the linear stability of the above basic state under the assumption of weak centrifugal force. The nondimensional velocity disturbances (u', v', w'), the density ρ', and the pressure perturbation p' are introduced as follows:

$$u=U+\gamma Lu', \tag{12}$$

$$v=V+\gamma Lv', \tag{13}$$

$$w=W+\gamma Lw', \tag{14}$$

$$\rho=\rho_0+\rho^* e^{-\alpha Lz}N^2\,\text{Fr}\,\rho', \tag{15}$$

$$p=P+\rho^*\gamma^2 L^2 e^{-\alpha Lz}p'. \tag{16}$$

Substituting (12)–(16) into (1)–(3) and discarding nonlinear terms as well as the higher-order terms in the Fr expansion, we have the following set of linearized equations:

$$D_t u' - (1+\varepsilon)v' = -\frac{\partial p'}{\partial x}, \tag{17}$$

$$D_t v' + (1-\varepsilon)u' = -\frac{\partial p'}{\partial y}, \tag{18}$$

$$D_t w' = -\frac{\partial p'}{\partial z} - N^2 \rho', \tag{19}$$

$$D_t \rho' - w' = 0, \tag{20}$$

$$\operatorname{div} \mathbf{u}' = 0, \tag{21}$$

where D_t denotes the Lagrangian derivative along the basic flow field:

$$D_t \equiv \frac{\partial}{\partial t} - (1+\varepsilon) y \frac{\partial}{\partial x} + (1-\varepsilon) x \frac{\partial}{\partial y}. \tag{22}$$

Let us consider the disturbances in the form assumed by Bayly,[9] Landman and Saffman,[10] Waleffe,[7] and Craik:[12]

$$\begin{pmatrix} u' \\ v' \\ w' \\ \rho' \end{pmatrix} = \begin{pmatrix} \hat{u} \\ \hat{v} \\ \hat{w} \\ \hat{\rho} \end{pmatrix} e^{i\mathbf{k}(t)\cdot\mathbf{x}} \tag{23}$$

and

$$D_t e^{i\mathbf{k}(t)\cdot\mathbf{x}} = 0. \tag{24}$$

Craik and Criminale[15] demonstrated that this class of solutions provides a new class of 3-D exact solutions of the Navier–Stokes equations under a more general situation, where spatially periodic disturbances are superimposed on a time-dependent uniform shear. As the basic shear considered here is time-independent, (24) can be solved easily to give

$$k_x = \kappa(1+\varepsilon)^{-1/2}(1-\varepsilon)^{1/2}\cos\varphi, \quad k_y = \kappa \sin\varphi, \quad k_z = \mu, \tag{25}$$

with

$$\varphi = (1-\varepsilon^2)^{1/2}(t-t_0), \tag{26}$$

where κ and μ are constants representing the magnitude of the wave number and φ is the normalized time variable with t_0 being a suitable origin. We see, however, that only the ratio between κ and μ is relevant since the problem is scale invariant, as is expected from (17)–(21). Then, we find it better to use an angle parameter θ in place of them:

$$\kappa = (1+\varepsilon)^{1/2}(1-\varepsilon)^{-1/2}\sin\theta, \quad \mu = \cos\theta. \tag{27}$$

Following the procedure by Waleffe,[7] we eliminate u', v', w', and p' from (17)–(21) and obtain the equation for ρ' as

$$\left[D_t \left(\frac{\partial^2}{\partial x^2} + \frac{\partial^2}{\partial y^2} + \frac{\partial^2}{\partial z^2} \right) D_t^2 + 4(1-\varepsilon^2) \frac{\partial^2}{\partial z^2} D_t + 4\varepsilon \frac{\partial^2}{\partial x\, \partial y} D_t^2 \right.$$
$$\left. + 4\varepsilon N^2 \frac{\partial^2}{\partial x\, \partial y} + N^2 D_t \left(\frac{\partial^2}{\partial x^2} + \frac{\partial^2}{\partial y^2} \right) \right] \rho' = 0. \tag{28}$$

Substitution of (24)–(27) into the above equation yields the equation describing the time evolution of the disturbance amplitude:

$$(1 - \varepsilon\cos^2\theta - \varepsilon\sin^2\theta\cos 2\varphi)\frac{d^3\hat{\rho}}{d\varphi^3}$$
$$+ 4\varepsilon\sin^2\theta\sin 2\varphi\frac{d^2\hat{\rho}}{d\varphi^2} + \left(4(1-\varepsilon)\cos^2\theta \right.$$
$$\left. + \frac{N^2}{1-\varepsilon^2}\sin^2\theta(1-\varepsilon\cos 2\varphi) \right)\frac{d\hat{\rho}}{d\varphi}$$
$$+ 4\varepsilon\sin^2\theta\frac{N^2}{1-\varepsilon^2}\sin 2\varphi\hat{\rho} = 0. \tag{29}$$

Thus the problem is reduced to a cubic-order Ince equation. Although (29) is convenient in discussing the physical mechanisms of the instability, we further cast it into a matrix form and deal with the matrix Floquet problem:

$$\frac{d}{d\varphi}\mathbf{M} = \begin{pmatrix} 0 & 1 & 0 \\ 0 & 0 & 1 \\ \xi & \eta & \zeta \end{pmatrix}\mathbf{M},$$

$$\xi = -\frac{4\varepsilon N^2 \sin^2\theta\sin 2\varphi}{(1-\varepsilon^2)(1-\varepsilon\cos^2\theta - \varepsilon\sin^2\theta\cos 2\varphi)},$$

$$\eta = -\frac{4(1-\varepsilon)^2(1+\varepsilon)\cos^2\theta + N^2\sin^2\theta(1-\varepsilon\cos 2\varphi)}{(1-\varepsilon^2)(1-\varepsilon\cos^2\theta - \varepsilon\sin^2\theta\cos 2\varphi)}, \tag{30}$$

$$\zeta = -\frac{4\varepsilon\sin^2\theta\sin 2\varphi}{1-\varepsilon\cos^2\theta - \varepsilon\sin^2\theta\cos 2\varphi},$$

where $\mathbf{M}$ is the solution matrix with $\mathbf{M}(0)$ being the unit matrix $\mathbf{I}_3$. The eigenvalues of $\mathbf{M}$ (2π) are the Floquet multipliers ν_i which determine the growth rate of the disturbance. We notice that one multiplier ν_3 (say) is unity and that the others ν_1 and ν_2 satisfy the relation $\nu_1 \cdot \nu_2 = 1$, with ν_i being complex conjugates of each other or real reciprocals. When the latter happens, the proper choice of growth rate is

$$\sigma = \frac{\sqrt{1-\varepsilon^2}}{2\pi}\log|\nu_1|, \tag{31}$$

where ν_1 is the multiplier with larger absolute value.

III. NUMERICAL RESULTS

The matrix $\mathbf{M}$ (2π) is computed numerically using the fourth-order Runge–Kutta–Gill method and its eigenvalues are determined by a standard mathematical package (double QR method). First, we reproduce the known results for the homogeneous case ($N=0$). Figure 1 depicts the contours of constant growth rate in the ε-θ plane, where the horizontal axis is the rate of strain ε and the vertical one denotes the angle θ between the wave-number vector and the vertical axis. The outermost contour traces the growth rate 10^{-5} and the inner lines correspond to the levels of 0.04, 0.08, 0.12, etc. The maximum growth rate 0.35 is attained at $\varepsilon = 0.81$, $\theta_{\max} = 0.83$. Similar figures showing the level curves of growth rate in the ε-θ plane are

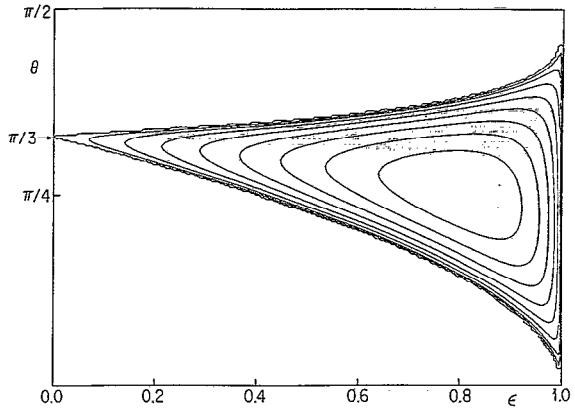

FIG. 1. Contour map of growth rate σ for $N=0.0$. The outermost line traces the growth rate 10^{-5}, and the contour interval is 0.04. The small-scale waviness of the lowest contour is due to the contouring routine.

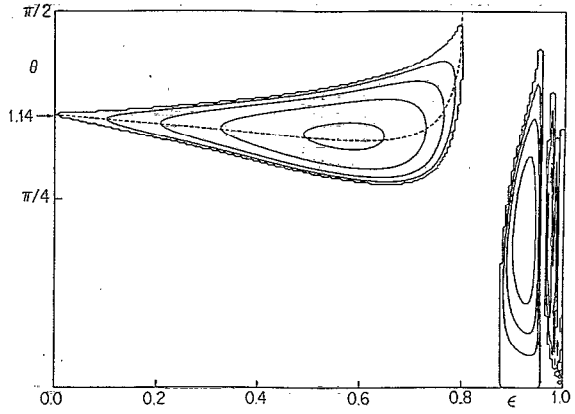

FIG. 3. Contour map of growth rate σ for $N=0.6$. The broken line shows the curve $\omega=1$ [see (43) in Sec. IV].

useful in distinguishing the types of instability when we consider the effect of stable stratification ($N>0$).

Our main findings are illustrated in Figs. 2–6. Each figure shows the contours of constant growth rate. The values of the Brunt–Väisälä frequency are increased as 0.3 (Fig. 2), 0.6 (Fig. 3), 0.9 (Fig. 4), 1.5 (Fig. 5), and 2.1 (Fig. 6).

We see in Fig. 2 that both the growth rate and the area of the parameter region where the instability occurs are diminished slightly. This result confirms our intuition that the stable stratification should work in the direction to suppress the 3-D instability mode. However, it is not the whole story. A different kind of instability manifests itself in the narrow region close to the line $\varepsilon=1$.

The suppression of the elliptical instability becomes more evident as the Brunt–Väisälä frequency is increased (Figs. 3 and 4). We notice that the parameter region is limited from right near the line $\varepsilon=(1-N^2)^{1/2}$ and then it disappears when the Brunt–Väisälä frequency exceeds unity (Fig. 5), i.e., the instability occurs only for $N^*=N/(1-\varepsilon^2)^{1/2}<1$. On the other hand, we find on the right side of the Figs. 3 and 4 that the new instability modes are classified into two types. Since the parameter N in (29) appears in the form $N^2/(1-\varepsilon^2)$ $(=N^{*2})$, we observe what occurs for very large values of N in the region near $\varepsilon=1$ and conversely we can clarify the fine structure near $\varepsilon=1$ by studying the case of larger N. The region of instability of the first kind extends to the left side of the line $\varepsilon=\varepsilon_c=(4-N^2)^{1/2}/2$ (shown by the vertical broken lines in Figs. 4 and 5), which corresponds to the condition of the parametric excitation of the internal gravity waves ($N^*=2$). It is likely that this instability stems from a related resonance phenomenon and we call it "the fundamental instability." But, a separate and more careful consideration incorporating some of the neglected physical factors, such as viscosity, diffusivity, higher-order centrifugal effects, and nonlinearity, is required in order to fully clarify the stability characteristics in the vicinity of the resonance line where the construction of the basic flow by the Fr expansion breaks down. The second type of instability has more complicated contour patterns in the ε-θ plane (Figs. 3–5). Several branches seem to emanate from the lower right corner $(\varepsilon,\theta)=(1,0)$. We call it "the superharmonic instability." Although it is difficult to ascertain from the figures, because of low resolution (200×200 mesh points), we show in the next section that there are an

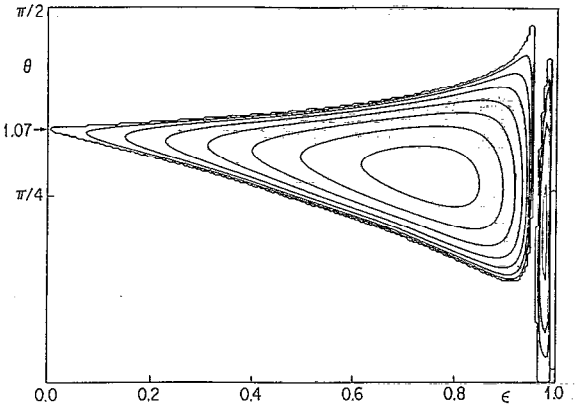

FIG. 2. Contour map of growth rate σ for $N=0.3$.

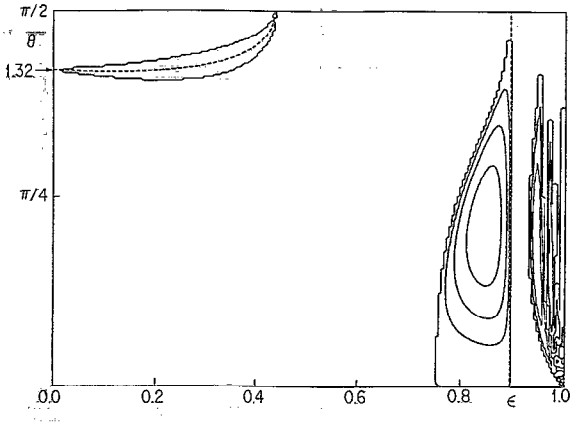

FIG. 4. Contour map of growth rate σ for $N=0.9$. The broken lines are the curves $\omega=1$ and $\omega=2$ [see (43) in Sec. IV].

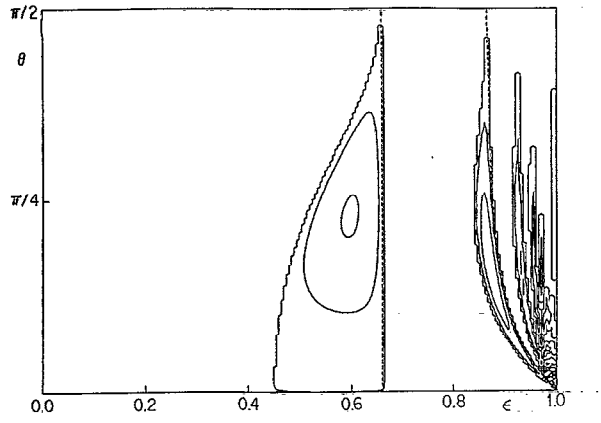

FIG. 5. Contour map of growth rate σ for $N=1.5$. The broken lines are the curves $\omega=2$ and $\omega=3$ [see (43) in Sec. IV].

infinite number of ranges. It is also noted that there are gaps separating the three instability regions (Figs. 3–5), where the elongated vortices are stable against any small disturbances.

As the Brunt–Väisälä frequency is raised further (Fig. 5), the parameter region of the fundamental instability moves to the left and it reaches the θ axis when $N=2$. Thus, only the superharmonic instability survives for N larger than 2 (Fig. 6). Its parameter region, also, develops more and more toward the left direction (smaller ε region) with the width of each range becoming narrower and the growth rate smaller, as the stable stratification becomes stronger. It is to be noted that the θ range of instability for a fixed ε is very narrow. The fact that the superharmonic instability is highly selective implies the existence of some underlying resonance phenomena. Detailed physical considerations on the appearance and disappearance of these instability modes are supplied in the following section. We sum up our findings as follows.

(a) The Pierrehumbert instability is weakened by the stable stratification effect and it vanishes if the Brunt–Väisälä frequency becomes greater than unity (or more strictly, it disappears for $N^*>1$).

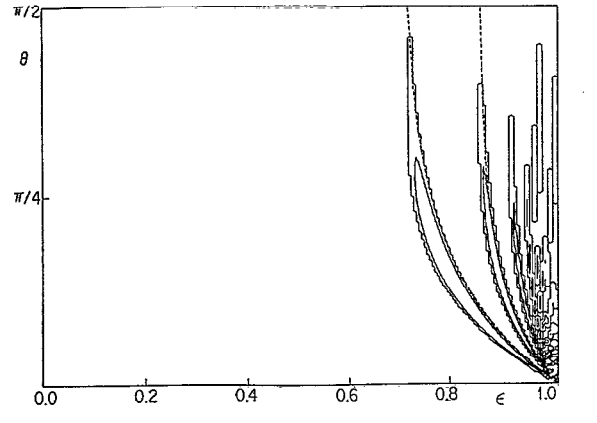

FIG. 6. Contour map of growth rate σ for $N=2.1$. The broken lines are the curves $\omega=3$ and $\omega=4$ [see (43) in Sec. IV].

(b) The fundamental instability is observed for $N<2$. Its parameter region of existence extends to the left side of the line of the critical strain $\varepsilon=\varepsilon_c=(4-N^2)^{1/2}/2$ $(N^*=2)$.

(c) The superharmonic instability persists for any values of N. Its parameter region emanates from $(\varepsilon,\theta)=(1,0)$ and extends as an infinite number of narrow ranges in the ε-θ plane.

Of these, (a) is consistent with the intuition but (b) and (c) are newly found. The next step is to inquire about their physical mechanisms.

IV. PHYSICAL CONSIDERATIONS

Waleffe[7] provided an illuminating physical interpretation of the elliptical instability (of unbounded vortices) in the limiting case of weak strain. Similar consideration is useful for understanding not only the mechanisms of its disappearance but also of the emergence of other instability modes. When $\varepsilon=0$ the basic state is one of pure rotation with the angular velocity 1. Then, a clearer picture will be available if we look at things from the coordinates rotating with the same angular velocity. In these coordinates, (17)–(21) are rewritten as

$$\frac{\partial u'}{\partial t}-2v'=-\frac{\partial p'}{\partial x}, \tag{32}$$

$$\frac{\partial v'}{\partial t}+2u'=-\frac{\partial p'}{\partial y}, \tag{33}$$

$$\frac{\partial w'}{\partial t}=-\frac{\partial p'}{\partial z}-N^2\rho', \tag{34}$$

$$\frac{\partial \rho'}{\partial t}-w'=0, \tag{35}$$

$$\operatorname{div}\mathbf{u}'=0, \tag{36}$$

where $-2v'$ in (32) and $2u'$ in (33) represent the Coriolis terms. We see that the plane wave perturbations

$$\begin{pmatrix}u'\\v'\\w'\\\rho'\end{pmatrix}=\begin{pmatrix}\bar{u}\\\bar{v}\\\bar{w}\\\bar{\rho}\end{pmatrix}e^{i(\mathbf{k}_0\cdot\mathbf{x}-\omega_0 t)},\quad \mathbf{k}_0=\begin{pmatrix}\sin\theta_0\cos\varphi_0\\\sin\theta_0\sin\varphi_0\\\cos\theta_0\end{pmatrix} \tag{37}$$

are permissible if the dispersion relation

$$\omega_0^2=N^2+(4-N^2)\cos^2\theta_0 \tag{38}$$

is fulfilled. If a steady strain field $\varepsilon\ll 1$ is superimposed in the inertial frame, it rotates with the angular velocity -1 in the rotating coordinates. Waleffe[7] demonstrated that a parametric excitation of the inertial wave occurs if the magnitude of its eigenfrequency is unity. This is the essence of the elliptical instability of Pierrehumbert type. In fact, the resonance condition is attained at $\theta_0=\pi/3$ in the homogeneous rotating flow $(N=0)$ and we can check in Fig. 1 that the parameter region of instability touches the θ axis at this point $(0,\pi/3)$. When the stably stratified fluid is taken into consideration, the resonance condition is superseded by

$$1=N^2+(4-N^2)\cos^2\theta_c. \tag{39}$$

The values of θ_c shown in Figs. 2–4, where the instability region reaches the θ axis, do satisfy the relation (39). This accounts for the reason why the instability region moves upwards as N is increased. If the Brunt–Väisälä frequency exceeds unity, (39) can never be attained and the elliptical instability of Pierrehumbert type is inhibited. The growth rate of the disturbances for small ε is computed by the method of multi-time-scale asymptotic expansions as

$$[9(1-N^2)/4(4-N^2)]\varepsilon. \tag{40}$$

The mathematical procedure is straightforward and we describe its outline in the Appendix. Note that the growth rate decreases with N and it vanishes at $N=1$.

A higher-order parametric excitation of inertial gravity waves is possible for an inhomogeneous fluid, if ω_0 is an integer larger than unity. For example, putting $N=2$ in (38), we obtain $\omega_0=2$ for any θ_0. This seems to be related with the fundamental instability, but physically more important is the fact that the parameter region of its existence is usually apart from the θ axis and limited from right near the line $\varepsilon=\varepsilon_c$ ($N^*=2$). As N increases to 2, the instability region between $\varepsilon=0$ and $\varepsilon=\varepsilon_c$ shrinks and disappears for N larger than 2. Hence it is natural to regard this instability as the result of the resonance between the internal gravity waves (pure buoyancy oscillations) and the elliptically rotating motion. This is the reason we call it "the fundamental instability." Unfortunately, we are not able to achieve the full understanding of it in the framework posed in this paper, since the basic flow cannot be well constructed near the critical line $\varepsilon=\varepsilon_c$.

If the Brunt–Väisälä frequency is increased over 3, substitution of $\theta_0=\theta_3=\cos^{-1}[(N^2-9)/(N^2-4)]^{1/2}$ into (38) gives $\omega_0=3$, indicating the occurrence of another higher-order resonance. In order to obtain a clearer view, we replotted the contours of constant growth rate in Figs. 7(a)–7(c) for $N=1.5$, 2.1, and 3.5, where the horizontal axis is $N^*=N/(1-\varepsilon^2)^{1/2}$ instead of ε. We find that the lowest branch in Fig. 7(c) stretches toward the line $N^*=3.5$ ($\varepsilon=0$) and we can confirm by a finer plot (not shown) that the instability branch does reach the line $\varepsilon=0$ at $\theta_3=0.892$ (the value obtained by putting $N=3.5$ in the above form). This observation tells why we call it "the superharmonic instability," i.e., it is caused by a higher-order parametric excitation of inertial gravity waves. We have seen in the previous section that the superharmonic instability occurs for any N (>0) and that every instability range comes out from the lower-right corner $(\varepsilon,\theta)=(1,0)$. It may seem strange to discuss its physical mechanisms in the weak strain limit, since no branch reaches the line $N^*=N$ ($\varepsilon=0$) for N less than 3. However, we would like to point out that every branch of the superharmonic instability shifts downwards and stretches toward the line $N^*=N$ ($\varepsilon=0$) *continuously* as the Brunt–Väisälä frequency is increased. We expect that the underlying mechanism is invariant during the change of N.

Further, it is seen in Figs. 7(a) and 7(b) that the branches of the superharmonic instability reach the line

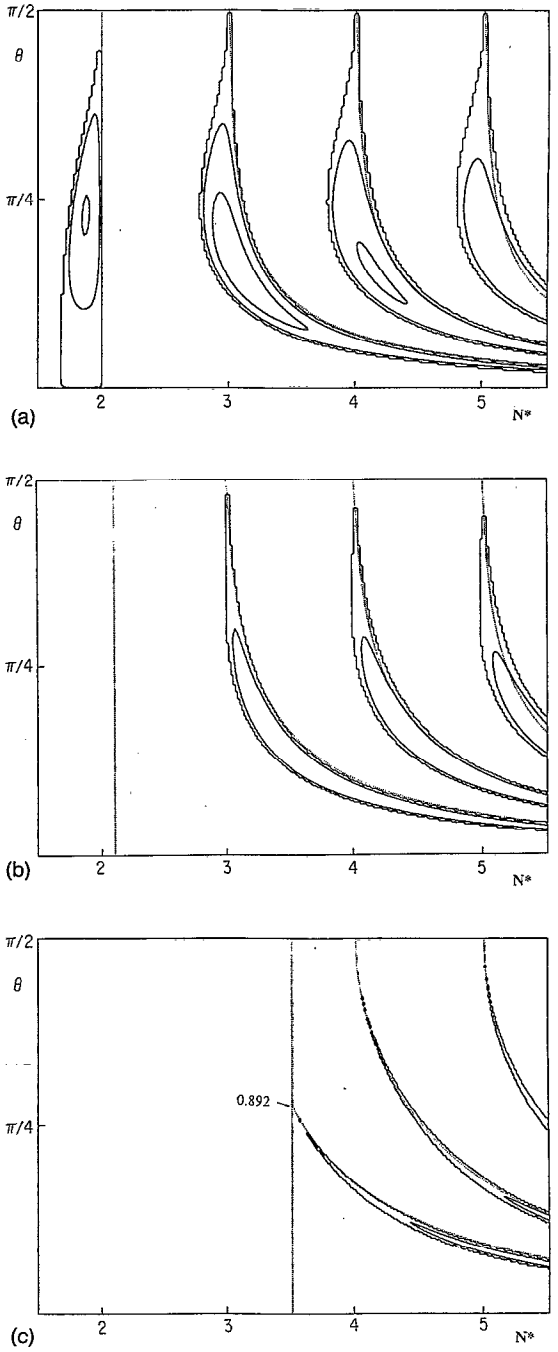

FIG. 7. (a) Contour map of growth rate σ in the N^*-θ plane for $N=1.5$. The broken lines are the curves $\omega=2$–5. (b) Contour map of growth rate σ in the N^*-θ plane for $N=2.1$. The broken lines are the curves $\omega=3$–5. (c) Contour map of growth rate σ in the N^*-θ plane for $N=3.5$. The broken lines are the curves $\omega=3$–5.

$\theta=\pi/2$ at $N^*=3$, 4, 5,... [in Fig. 7(c) $N^*=4$, 5,...], indicating higher-order resonance phenomena. Thus, the physical origin of the superharmonic instability is the higher-order parametric excitation of inertial gravity waves (note that inertial gravity waves reduce to pure buoyancy oscillations in the parameter region near $\theta=\pi/2$) and there is an infinite number of branches corresponding to the inertial gravity wave modes whose eigenfrequencies, in the weak strain limit, are integers greater than 2.

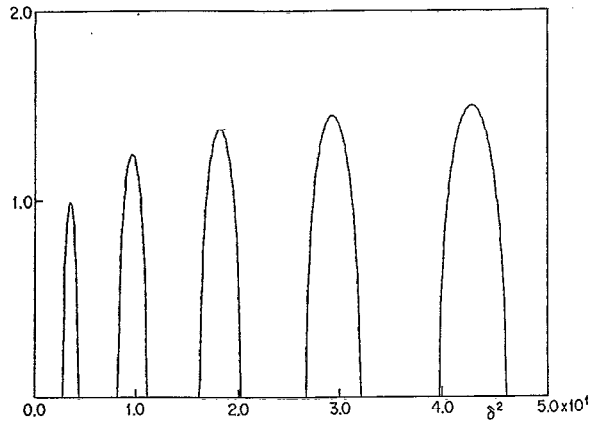

FIG. 8. Coefficient of the growth rate in the limit $(\varepsilon,\theta)\to(1,0)$.

The latter part of the above statement is reinforced by examining in detail the limit of $(\varepsilon,\theta)\to(1,0)$, from where all instability ranges emanate. In this limit, (29) is reduced to

$$\frac{d^3\hat{\rho}}{d\varphi^3}+[4+\delta^2(1-\cos 2\varphi)]\frac{d\hat{\rho}}{d\varphi}+4\delta^2\sin 2\varphi\hat{\rho}=0, \quad (41)$$

where we introduced the variable δ^2 by

$$\delta^2=(N^2\sin^2\theta)/2(1-\varepsilon)^2 \quad (42)$$

and we assumed it to be order of unity. The Floquet exponents associated with the cubic Ince equation (41) are calculated numerically, as in the previous section. The growth rate is proportional to $(1-\varepsilon^2)^{1/2}$ and its coefficient is plotted as a function of δ^2 in Fig. 8. There appears a series of separate instability bands. Although this is not a mathematical proof, it tells us that many narrow branches are, actually, stretching out from the corner (1,0) for all N (>0).

In addition to these discussions for the limiting cases of weak strain, of $\theta\to\pi/2$ and of $(\varepsilon,\theta)\to(1,0)$, one of the referees suggested the way to observe a more direct relation between instabilities and resonance phenomena. We notice the important frequency inherent in (29)

$$\omega^2=\frac{4(1-\varepsilon)\cos^2\theta+N^{*2}\sin^2\theta}{1-\varepsilon\cos^2\theta}, \quad (43)$$

which is the ratio of the coefficient of the first-order differential term to that of the third-order differential term [averaged over one period of φ: see also Eq. (A2)]. It tends to ω_0^2 (38) as $\varepsilon\to 0$ and to N^{*2} as $\theta\to\pi/2$. A resonance will be expected if this frequency coincides with an integer. We plotted the resonance curves $\omega=1$ (broken lines in Figs. 3 and 4), $\omega=2$ [$\varepsilon=\varepsilon_c$: Figs. 4, 5, and 7(a)], $\omega=3$ (Figs. 5–7), $\omega=4$ (Figs. 6 and 7), and $\omega=5$ [Figs. 7(a)–7(c)]. In every case, the close link between instability and resonance is ascertained. Thus, the interpretation of the instabilities as the resonance phenomena associated with inertial gravity waves is confirmed. It may be better to call the Pierrehumbert instability "the subharmonic instability,"

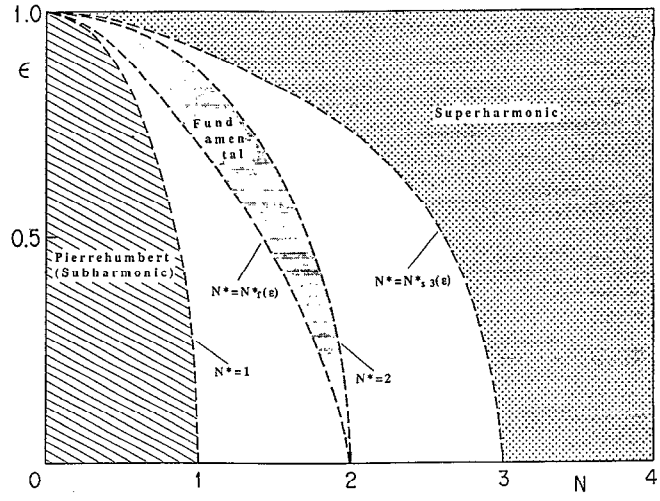

Stability diagram in the N-ε plane. The Pierrehumbert (subharmonic) instability occurs for $N^*<1$, the fundamental instability for $N_f^*(\varepsilon)<N^*<2$ and the supurharmonic instability for $N^*>N_{s3}^*(\varepsilon)\approx 3$.

following the names ("the fundamental and superharmonic instabilities") of other instability modes.

Finally, we show in Fig. 9 the instability diagram in the N-ε plane, where the abscissa denotes the Brunt–Väisälä frequency N and the ordinate is the rate of strain ε. The regions of the three instability modes are hatched differently. The parameter region of the Pierrehumbert instability (the subharmonic instability) is limited by the line $N^*=N/(1-\varepsilon^2)^{1/2}=1$ and that of the fundamental instability is limited from right near the line $N^*=2$. When N is less than 1, a strained vortex is unstable to one of three instability modes depending on its ellipticity ε. It is noted that there are gaps between each instability region and that the vortices in these gaps are stable against any small perturbation. When N lies between 1 and 2, the elliptic vortex is unstable to the fundamental $[N_f^*(\varepsilon)<N^*<2]$ or the superharmonic instability $[N^*>N_{s3}^*\approx 3: N_{s3}^*(\varepsilon)$ is slightly less than 3]. Again, there are two stable regions. One includes N axis, i.e., small ε, and the other lies between the two instability regions. When N is larger than 2, only the superharmonic instability is observed for $N^*>N_{s3}^*(\varepsilon)$. The stable region remaining near the N axis vanishes, if N is increased over 3. It then implies that any strained vortex is unstable to the superharmonic instability (at least, the $\omega=3$ mode is presented) under strong stratification but that the maximum growth rate for a fixed strain rate decreases rapidly as N increases.

V. SUMMARY AND DISCUSSIONS

In this paper, we have investigated the effect of stable density stratification on the 3-D short wave instability of strained vortices. The fluid is assumed to be inviscid, incompressible, nondiffusive, and exponentially stratified.

The elliptical instability of Pierrehumbert type (the subharmonic instability) is shown to be suppressed by the stratification effect and it is eliminated when the Brunt–Väisälä frequency $N=(\alpha g)^{1/2}/\gamma$ is greater than unity [more strictly $N^*=N/(1-\varepsilon^2)^{1/2}>1$], whereas two classes

of the new instability mode are found to exist. The fundamental instability occurs if the Brunt–Väisälä frequency N is less than 2. Its parameter region of existence in the ε-θ plane suggests its close link with a parametric excitation of the internal gravity wave. However, our analysis based on the assumption of weak centrifugal force is invalidated near the critical line $\varepsilon=\varepsilon_c$ ($N^*=2$) and a full understanding of this mode is left for future work. The superharmonic instability is found for any positive Brunt–Väisälä frequency. This instability is allowed only for strongly strained vortices [for $N^* > N_{s3}^*(\varepsilon)$] if N is less than 3, while all elliptical vortices become unstable if N is larger than 3. It is tied to the higher-order resonances between inertial gravity waves and the imposed strain field. Its parameter region of occurrence in the ε-θ plane is characterized by an infinite number of narrow branches stretching out from the corner $(\varepsilon,\theta)=(1,0)$.

We have revealed in this paper that the density stratification has a nontrivial effect on the stability of strained vortices and that 3-D instability modes persist even in the presence of stable density stratification. Although our study is limited to the highly idealized case, it might provide some insight on transition to turbulence in a stably stratified fluid.

ACKNOWLEDGMENT

The authors wish to thank the referees for their helpful comments, especially for pointing out the importance of the frequency ω in (43).

APPENDIX: DERIVATION OF (40)

Analytical results based on a multiple time-scale expansion method are described for the limiting case of weak ellipticity $\varepsilon \ll 1$. We introduce a new parameter θ' instead of θ, for brevity:

$$\tan\theta'=(1-\varepsilon)^{-1/2}\tan\theta. \tag{A1}$$

They coincide in the limit $\varepsilon\to 0$. Equation (29) is rewritten as

$$(1-\varepsilon\sin^2\theta'\cos 2\varphi)\frac{d^3\hat{\rho}}{d\varphi^3}+4\varepsilon\sin^2\theta'\sin 2\varphi\frac{d^2\hat{\rho}}{d\varphi^2}+\left(4\cos^2\theta'+\frac{N^2}{1-\varepsilon^2}\sin^2\theta'(1-\varepsilon\cos 2\varphi)\right)\frac{d\hat{\rho}}{d\varphi}+\frac{4\varepsilon N^2\sin^2\theta'}{1-\varepsilon^2}\sin 2\varphi\hat{\rho}=0. \tag{A2}$$

Substitution of the series expansion

$$\hat{\rho}=\hat{\rho}_0+\varepsilon\hat{\rho}_1+\cdots \tag{A3}$$

into (A2) yields the following linear equation, at the zeroth order:

$$\frac{d^3\hat{\rho}_0}{d\varphi^3}+\omega_0^2\frac{d\hat{\rho}_0}{d\varphi}=0 \tag{A4}$$

with

$$\omega_0^2=4\cos^2\theta'+N^2\sin^2\theta'. \tag{A5}$$

Remember that (A5) is identical with the dispersion relation (38) of inertial gravity waves in a stably stratified fluid rotating rigidly. The first-order equation is inhomogeneous:

$$\frac{d^3\hat{\rho}_1}{d\varphi^3}+\omega_0^2\frac{d\hat{\rho}_1}{d\varphi}=\sin^2\theta'\cos 2\varphi\frac{d^3\hat{\rho}_0}{d\varphi^3}-4\sin^2\theta'\times\sin 2\varphi\frac{d^2\hat{\rho}_0}{d\varphi^2}+N^2\sin^2\theta'\cos 2\varphi\frac{d\hat{\rho}_0}{d\varphi}-4N^2\sin^2\theta'\sin 2\varphi\hat{\rho}_0. \tag{A6}$$

It is seen easily that a resonance occurs if $\omega_0^2=1$. In order to remove the secular terms on the right-hand side, we allow for a slow time evolution of the amplitudes of the zeroth-order terms:

$$\hat{\rho}_0=A(\varepsilon\varphi)\cos\varphi+B(\varepsilon\varphi)\sin\varphi. \tag{A7}$$

Then two inhomogeneous terms $-2A\sin\varphi$ and $2B\cos\varphi$ are added to the right-hand side of (A6) and we find, from the solvability condition, that

$$\dot{A}=-3/4\sin^2\theta'(1-N^2)B, \tag{A8}$$

$$\dot{B}=-3/4\sin^2\theta'(1-N^2)A. \tag{A9}$$

Finally, we obtain the growth rate (40) using (A8), (A9) with (A5), and $\omega_0^2=1$.

[1]S. C. Crow, "Stability theory for a pair of trailing vortices," AIAA J. **8**, 2172 (1970).
[2]S. E. Widnall, D. B. Bliss, and C. Y. Tsai, "The instability of short waves on a vortex ring," J. Fluid Mech. **66**, 35 (1974).
[3]R. T. Pierrehumbert, "Universal short-wave instability of two-dimensional eddies in an inviscid fluid," Phys. Rev. Lett. **57**, 2157 (1986).
[4]C. Y. Tsai and S. E. Widnall, "The stability of short waves on a straight vortex filament in a weak externally imposed strain field," J. Fluid Mech. **73**, 721 (1976).
[5]D. W. Moore and P. G. Saffman, "The instability of a straight vortex filament in a strain field," Proc. R. Soc. London Ser. A **346**, 415 (1975).
[6]Ye. B. Gledzer, F. V. Dolzhanskiy, A. M. Obukhov, and V. M. Pomonarev, "An experimental and theoretical study of the stability of motion of a liquid in an elliptical cylinder," Izv. Acad. Sci. USSR Atmos. Oceanic Phys. **11**, 981 (1975).
[7]F. Waleffe, "On the three-dimensional instability of strained vortices," Phys. Fluids A **2**, 76 (1990).
[8]Malkus and F. Waleffe, "Transition from order to disorder in elliptical flow: A direct path to shear flow turbulence," *Advances in Turbulence 3*, Proceedings of the 3rd European Turbulence Conference (Springer-Verlag, Berlin, 1991), p. 197.
[9]B. J. Bayly, "Three-dimensional instability of elliptical flow," Phys. Rev. Lett. **57**, 2160 (1986).
[10]M. J. Landman and P. G. Saffman, "The three-dimensional instability of strained vortices in a viscous fluid," Phys. Fluids **30**, 2339 (1987).
[11]S. A. Orszag and A. Patera, "Secondary instability of wall-bounded shear flows," J. Fluid Mech. **128**, 347 (1983).
[12]A. D. D. Craik, "The stability of unbounded two- and three-dimensional flows subject to body forces: Some exact solutions," J. Fluid Mech. **198**, 275 (1989).
[13]T. Miyazaki and Y. Fukumoto, "Axisymmetric waves on a vertical vortex in a stratified fluid," Phys. Fluids A **3**, 606 (1991).
[14]R. W. Griffiths and P. F. Linden, "The stability of vortices in a rotating stratified fluid," J. Fluid Mech. **105**, 283 (1981).
[15]A. D. D. Craik and W. O. Criminale, "Evolution of wavelike disturbances in shear flows: A class of exact solutions of the Navier–Stokes equations," Proc. R. Soc. London Ser. A **406**, 13 (1986).